Available online at www.sciencedirect.com
ScienceDirect
Energy Reports 6 (2020) 885–890
www.elsevier.com/locate/egyr

6th International Conference on Energy and Environment Research, ICEER 2019, 22–25 July, University of Aveiro, Portugal

Oleic acid enhances the production of reactive oxygen species in neuronal tissue

J.L. Alves[a,*], A.S.C. Figueira[a], M. Souto[a], I.L. Lopes[b], J.C. Dionísio[c], R.M. Quinta-Ferreira[b], M.E. Quinta-Ferreira[d]

[a] *Department of Life Sciences, University of Coimbra, Calçada Martim de Freitas 3000-456, Coimbra, Portugal*
[b] *CIEPQPF — Chemical Engineering Processes and Forest Products Research Center, Department of Chemical Engineering, University of Coimbra, Rua Sílvio Lima, Coimbra – 3030-790, Portugal*
[c] *Department of Animal Biology, University of Lisbon, P-1749-016, Lisbon, Portugal*
[d] *CNC — Center for Neurosciences and Cell Biology, and Physics Department, University of Coimbra, Rua Larga, Coimbra – 3004-516, Portugal*

Received 19 November 2019; accepted 22 November 2019

Abstract

One of the major current goals is to obtain clean energy sources and to replace petroleum-derived fuel by biodiesel, which is made from biodegradable and renewable biomass such as vegetable oils. In particular, olive oil contains large amounts of oleic acid (OA), which is a monounsaturated fatty acid used for energy production and also for biosensors, nutritional products, pharmaceuticals and cosmetics. Since oleic acid is particularly abundant in olive oil, large concentrations of this fatty acid may exist in the effluents of olive mill production units, which need to be treated in order to avoid water contaminations and undesirable effects in the ecosystem. Indeed, this type of organic waste, which is potentially useful in the production of biodiesel, in excess may be toxic and cause neurodegeneration, through the production of cellular reactive oxygen species (ROS). The effect of 10–100 μM of oleic acid on neuronal ROS production was evaluated in brain slices incubated with the permeant fluorescent ROS indicator H_2DCFDA. The experiments revealed that the amplitude of the ROS signals, corrected for the autofluorescence, increased slightly for the OA concentrations in the range 60–100 μM.

Peer-review under responsibility of the scientific committee of the 6th International Conference on Energy and Environment Research, ICEER 2019.

Keywords: Autofluorescence; Biomass; H_2DCFDA indicator; Hippocampal CA3 area; Oleic acid; ROS

1. Introduction

Biodiesel is more beneficial than petroleum-derived fuel, from the environment point of view, because it is biodegradable and non-polluting and is produced from biomass sources consisting of vegetable oils, including waste cooking oils, animal fats and algae [1,2], which are renewable. The current methods used in its production,

* Corresponding author.
E-mail address: alvesjlr@hotmail.com (J.L. Alves).

https://doi.org/10.1016/j.egyr.2019.11.034

Peer-review under responsibility of the scientific committee of the 6th International Conference on Energy and Environment Research, ICEER 2019.

by transesterification processes, are mediated by alkaline, acidic or enzymatic catalysts. These processes may be expensive and/or not environmental friendly, existing a large interest in improving specially the latter one [2]. From the vegetable oils, olive oil is composed mainly of oleic acid (OA) that is a monounsaturated fatty acid (MUFA) with great nutritional value [3]. Thus, the effluents of olive mill production units are susceptible to having large concentrations of this fatty acid and even the sewers can be contaminated with cooking oils from houses [4].

Although OA is considered to provide a lot of benefits, as part of the Mediterranean diet, it can be harmful when consumed in large amounts [3,5,6]. In fact, previous studies indicated OA as a highly toxic compound to microorganisms, which results in difficulties in the treatment of olive mill wastewaters [7,8]. Residues coming from olive oil production are of special concern due to their potentially toxic composition, which causes, in large concentrations, adverse effects to ecosystems. Within these, the olive mill wastewater (gray waters) and the wet pomace should be stressed as sources of oleic acid, which show high potential to be used in other industries [9]. For these reasons it is important to investigate possible effects in biological systems, associated with an eventual exposure to this substance.

OA is thought to be involved in the formation of cellular reactive oxygen species (ROS). It can modulate NMDA channels (that are related to functions such as neural plasticity, memory and cognition), activate PKC that is a protein responsible for the phosphorylation of other proteins, and be oxidized in the Krebs cycle [10–13]. ROS play an important role in various mechanisms in the organism. However, when present in elevated intracellular amounts they can be neurotoxic and cause neurodegeneration [14]. Therefore, the presence of oleic acid in effluents generates a major concern for human health.

The aim of this work was to investigate the effect of OA on neuronal ROS formation in the hippocampal CA3 area. To assess the neurotoxicity, hippocampal slices were perfused with different concentrations of OA and fluorescence signals were measured using the fluorescent ROS indicator H_2DCFDA. Autofluorescence signals originating from flavoproteins activity in the mitochondria, were also measured and were used to correct the total fluorescence signals detected in incubated slices.

Oleic acid has many current applications and more are being found in connection to a wide variety of areas, including cosmetics, pharmaceuticals and biosensors [15,16], and the optimization of methane and energy production such as biodiesel [17–19].

2. Materials and methods

Hippocampal slices were prepared from pregnant Wistar rats (8–16 weeks old; 16–18 days of gestation) sacrificed by cervical dislocation under anaesthesia. Transverse slices (400 μm thick) were placed in an oxygenated (95% O_2, 5% CO_2) artificial cerebrospinal fluid (ACSF) prepared with ultrapure water and containing (in mM): 124.0 NaCl, 3.5 KCl, 24 $NaHCO_3$, 1.25 NaH_2PO_4, 2.0 $CaCl_2$, 2.0 $MgCl_2$, 10.0 D-glucose. Some slices were incubated (1 h) in an oxygenated ACSF solution containing the cell-permeant ROS indicator H_2DCFDA (2′,7′-dichlorodihydrofluorescein diacetate), at 20 mM. For the experiments, the slices were moved into an immersion-type recording chamber and were perfused at a rate of 1.5–2 mL/min with an oxygenated medium, at 32 °C. Different OA concentrations (10 μM, 20 μM, 40 μM, 60 μM and 100 μM) were applied. A stock solution of oleic acid (10 mM) was prepared by adding 4.7 μL of oleic acid in ultra-pure ethanol (100%) under a nitrogen atmosphere, applied for 3 min. Several vials of 1.5 mL were prepared and stored in the fridge, protected from the light, and when opened were only used once. The final solutions were prepared diluting a certain volume of the oleic acid stock solution in ACSF.

The optical signals were recorded using a fluorescence microscope (Zeiss, Axioskop), equipped with a tungsten/halogen lamp (12 V, 100 W) and a silicon photodiode (Hamamatsu, 1 mm^2). The light was focused at the preparation by means of a water immersion lens (40x, N.A. 0.75; working distance, 1.6 mm), targeted to the CA3 region of the hippocampal slice. The excitation and emission wavelengths were selected through a 480 nm narrow band (10 nm) interference filter and a high pass (>500 nm) emission filter, respectively.

The signals were obtained using a 16 bit A/D converter (National Instruments) and processed with the software Signal Express (National Instruments). The data were normalized by the average of the 10 baseline points. The points in the graphs correspond to the results of various experiments and represent the mean ± S.E.M. Data acquisition was made recording 100 points per minute and plotting only their mean value.

Drugs used were NaCl, KCl, $NaHCO_3$, NaH_2PO_4, $CaCl_2$, $MgCl_2$, D-glucose, Oleic acid (Sigma-Aldrich) and H_2DCFDA (Invitrogen by Thermo Fisher Scientific).

All experiments were carried out in accordance with the Directive 2010/63/EU of the European Parliament and Council. All efforts were made to minimize animal suffering and to use only the number of animals necessary to produce reliable scientific data.

3. Results and discussion

The effects of oleic acid, a major constituent of olive oil, found in abundance in olive mill wastewaters, were determined through optical recordings. These were performed in the mossy fibers-CA3 pyramidal cells synaptic system of hippocampal slices, using the fluorescence ROS indicator H_2DCFDA. The data are represented, at 1 min intervals, in the figures, where the first 10 points in ACSF form the baseline. In this study, fluorescence changes evoked by the application of OA were measured both from nonincubated and from H_2DCFDA loaded slices.

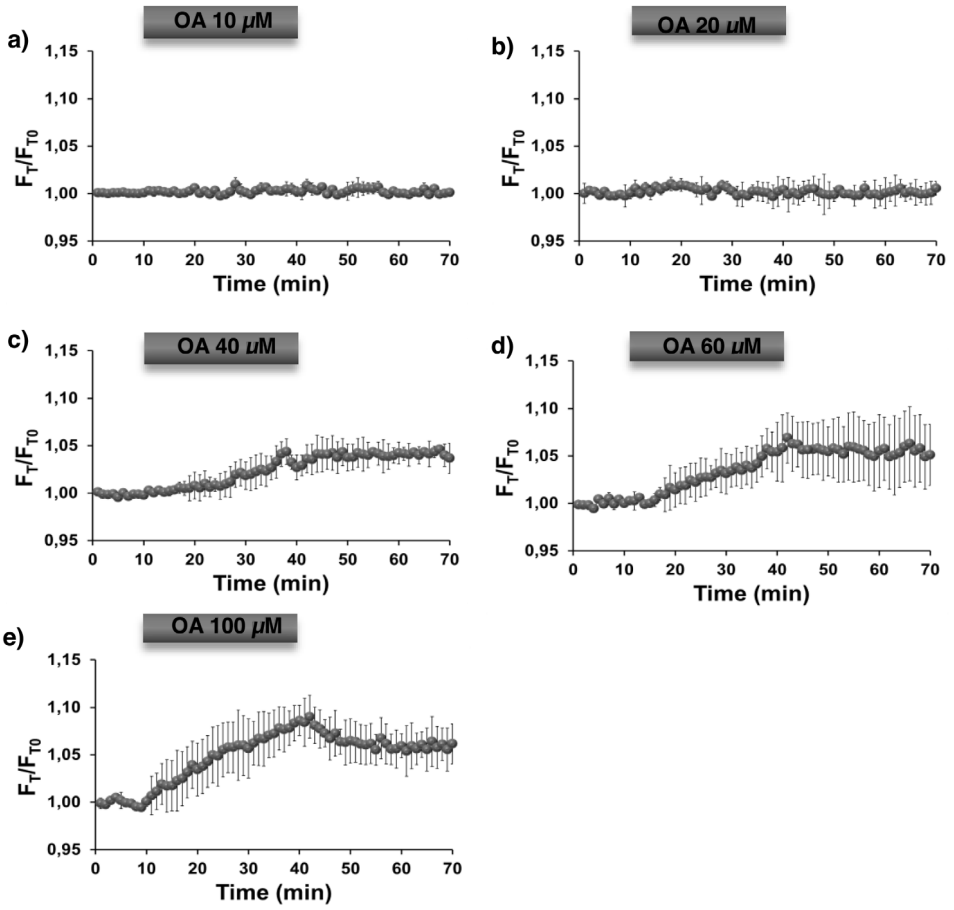

Fig. 1. Fluorescence signal obtained with H_2DCFDA, for different concentrations of OA applied in a neuronal system. a. 10 μM OA (n = 3), b. 20 μM OA (n = 3), c. 40 μM OA (n = 3), d. 60 μM OA (n = 3). e. 100 μM OA (n = 3). All values were normalized by the average of the first 10 responses and represent the mean ± SEM. F_T/F_{T0}, F_T, total fluorescence, F_{T0}, basal total fluorescence.

Taking into account the spectral characteristics of the intrinsic fluorescence of FAD and of ROS-H_2DCDFA complexes, the fluorescence signals obtained from slices incubated in H_2DCFDA, using excitation light of 480 nm and recording above 500 nm, have two different components: autofluorescence and the fluorescence of the ROS-H_2DCDFA complexes. The combined signals (total fluorescence), can be observed in Fig. 1, for different concentrations of OA. The amplitude of the optical responses increases with the OA concentration being only significant for the 40 μM, 60 μM and 100 μM OA media. In these cases, the signals become irreversibly potentiated since they do not recover upon removal of the OA solutions.

Thus, in the presence of 10 μM (Fig. 1a) and 20 μM (Fig. 1b) OA, the signals remained close to the baseline level. The perfusion of the 40 μM OA medium caused a rise in the total fluorescence (F_T) signals of 4.6 ± 1.5% of control, in the period 10–40 min (Fig. 1c) and in the final 30 min, corresponding to the second application of ACSF, the signal is maintained at the same level. In the presence of 60 μM OA (Fig. 1d) there was a higher enhancement

of the ROS signals, of 5.7 ± 1.7% in the period 40–70 min. The application of 100 μM OA (Fig. 1e) reveals a similar behavior to that observed for the 40 μM and 60 μM OA, with a maximum rise of 8.6 ± 1.2% and a partial recovery upon returning to ACSF, to approximately the same values as with 60 μM OA (Fig. 1d).

The characterization of autofluorescence has been largely addressed in fluorimetric studies performed in cultured cells or in monolayers incubated with an indicator. However, the situation is very different in brain slices, with widths ranging from about 300 to 400 nm, due to their thickness. In these cases, the large number of cells in the optical path leads to large autofluorescence changes that can mask significantly the dye-associated signals. Usually, that component, which is evaluated in the region of interest of non-incubated slices, is considered constant, being the same value subtracted from all raw fluorescence data points. However, the time varying nature of autofluorescence in brain slices has already been pointed out and needs to be taken into account in the correction procedure [20].

In this study autofluorescence signals (F_A) were recorded for the OA concentrations corresponding to the larger signals (60 μM and 100 μM OA) (Fig. 2a and c) and subtracted point to point from the corresponding signals in Fig. 1. These analysis was thus designed to extract the real ROS signals, shown in Fig. 2b and d, from the recorded signals obtained from the incubated slices.

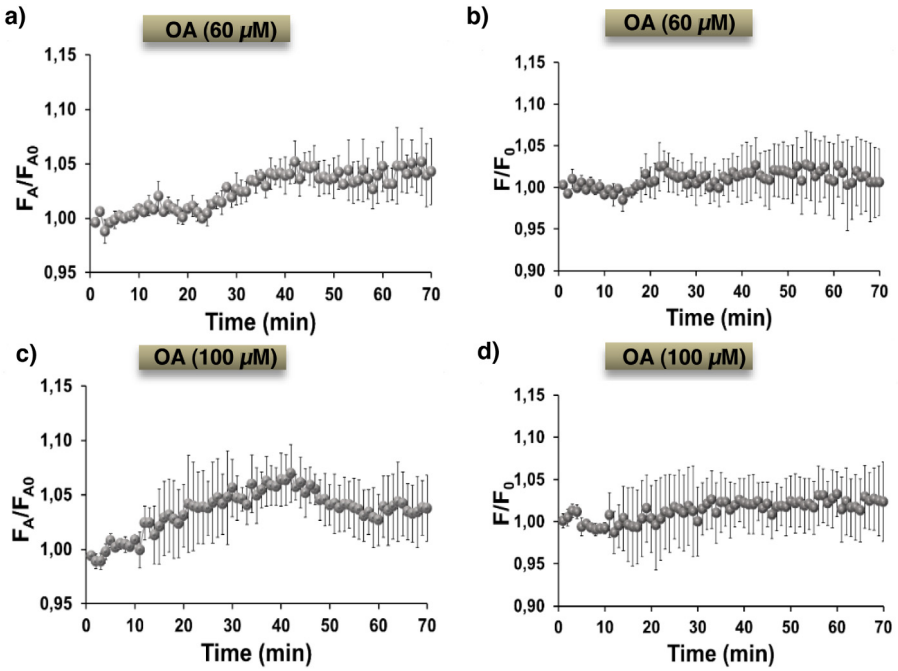

Fig. 2. Autofluorescence and ROS signals evoked by OA. a. 60 μM induced changes in autofluorescence (n = 2). b. ROS signals obtained as the difference between data in Fig. 1 and in the panel a. c. 100 μM OA induced changes in autofluorescence (n = 3) d. ROS signals obtained as the difference between data in Fig. 1 and in the c panel. The application of OA (60 μM and 100 μM) was made at the times indicated by the bars. All values were normalized by the average of the first 10 responses and represent the mean ± SEM. F_A, autofluorescence; F, fluorescence of the ROS signals; F_{A0}, F_0 basal auto and ROS fluorescences, respectively.

The autofluorescence data (Fig. 2a and c) reveal that the OA (60 μM and 100 μM) solutions cause an increase of the signals of 4.1 ± 1.4% and 6.2 ± 2.3, respectively, above baseline, in the period 35–40 min. The autofluorescence traces for these two OA concentrations showed a similar time course to that of the corresponding total fluorescence records (Fig. 1d, e) but with about half the amplitude (5% and 10% increases, respectively).

Thus, it can be observed that the ROS signals obtained after correcting the total fluorescence traces for the autofluorescence (Fig. 2b and d) had changes measuring about 2% and 3% in the cases of the 60 μM and 100 μM OA concentrations, respectively. It can also be noticed that these signals do not recover following the removal of OA. and that the larger component of the total fluorescence is autofluorescence.

OA can modulate NMDA channels leading to an influx of calcium that may cause an increase in the production of ROS such as hydrogen peroxide, through mitochondria and ROS generating enzymes [21,22]. The amount of

calcium entry is related to the intensity of autofluorescence because increased intracellular calcium can trigger an increase in FAD (flavoprotein) and NAD, as well as in the oxidation of $FADH_2$ and NADH [23–25]. Considering the spectral properties of FAD, since an excitation filter of 480 nm was used, being the emission light collected above 500 nm, the autofluorescence signals detected should have essentially flavoprotein origin. The redox couple $FAD/FADH_2$ operates in the citric acid cycle and respiratory chain, and it is therefore of no surprise that, at least in neuronal tissues, this autofluorescence component might originate mostly, if not exclusively from mitochondria [26–28].

Consequently, hydrogen peroxide, one type of postsynaptic ROS can travel and activate presynaptic PKCs, which OA can also activate. This may lead to an increase of the calcium influx and the release of more glutamate, causing the induction of a potentiation [10–13,29] as was observed during the application of the second ACSF. in both experiments. Furthermore, the activation of PKC by superoxide or OA resulting in higher glutamate release could explain the maintenance of the ROS signals observed upon washout (Figs. 1 and 2). The origin of the observed ROS signals is considered to have essentially a postsynaptic origin, since presynaptic mitochondria are smaller in diameter than postsynaptic mitochondria [30].

The observed enhancements of low concentrations, in the micromolar range, of oleic acid on both the autofluorescence and true ROS signals, draw the attention for the need to reduce the organic load of the olive mill wastewaters, part of which may be used for biodiesel production.

4. Conclusions

The set of experiments related to the induction of neuronal ROS changes by OA revealed total fluorescence signals with two components: autofluorescence and the fluorescence of the ROS-H_2DCDFA complex. The activation of NMDA channels leads to calcium influx and consequently to an increase in ROS production. PKC in the postsynaptic region can be activated both by ROS and by OA. The same protein can also be activated in the presynaptic region by ROS traveling from the postsynaptic area. This leads to an increase in the release of glutamate which can explain the irreversible part of the signals.

This study serves to reinforce the idea of the need to improve the methods of treatment of mill waste waters as low OA concentrations (micromolar) may induce damage in ecosystems by, for example, the production of ROS in animals and other living beings, which can cause disease. Gray waters are the main environmental problems caused by olive production industries, as the forms of treatment of those effluents are not efficient or viable in economic terms, leading to its unload in the environment [9]. The recovery of substances with increased value from olive mill wastewaters leads to a decrease in the organic pollutant load and can be a profitable activity since those substances may be used to produce biodiesel and increase the efficiency of other industrial processes like methane production [17,19]. The demand for cleaner and non-toxic fuels, in order to decrease the CO_2emissions and environmental pollution, called the attention to oleic acid enriched vegetable oils, which have a great potential in biodiesel production.

Acknowledgments

We thank CNC — Center for Neuroscience and Cell Biology, University of Coimbra, Coimbra, Portugal, for providing the rat brains.

Funding

Work funded by strategic project, Portugal UID/NEU/04539/2013.

References

[1] Khaligh G, Hamid S, Mihankhah T. Eco-friendly biodiesel production from waste olive oil by transesterification using nano-tube TiO2. Technology 2015;99(2008):3975–81. http://dx.doi.org/10.15242/IICBE.C0615102.

[2] Ranganathan S, Narasimhan S, Muthukumar K. An overview of enzymatic production of biodiesel. Bioresour Technol 2008;99(10):3975–81. http://dx.doi.org/10.1016/j.biortech.2007.04.060.

[3] Covas MI. Olive oil and the cardiovascular system. Pharmacol Res 2007;55(3):175–86. http://dx.doi.org/10.1016/j.phrs.2007.01.010.

[4] Bodzek M, Lobos-Moysa E, Zamorowska M. Removal of organic compounds from municipal landfill leachate in a membrane bioreactor, Vol. 198. Elsevier B.V; 2006, p. 16–23. http://dx.doi.org/10.1016/j.desal.2006.09.004.

[5] Carrillo C, Cavia MD, Alonso-Torre S. Role of oleic acid in immune system; mechanism of action; a review. Nutr Hosp 2012;27(4):978–90. http://dx.doi.org/10.3305/nh.2012.27.4.5783.
[6] Carrillo C, Cavia MD, Alonso-Torre SR. Antitumor effect of oleic acid; mechanisms of action; a review. Nutr Hosp 2012;27(6):1860–5. http://dx.doi.org/10.3305/nh.2012.27.6.6010.
[7] Hamdi M. Toxicity and biodegradability of olive mill wastewaters in batch anaerobic digestion. Appl Biochem Biotechnol 1992;37(155). http://dx.doi.org/10.1007/BF02921667.
[8] Kavvadias V, Doula MK, Komnitsas K, Liakopoulou N. Disposal of olive oil mill wastes in evaporation ponds: effects on soil properties. J Hard Mater 2010;182:144–55.
[9] Martins D. Valorização de resíduos da indústria doazeite: análise do potencial da recuperação de antioxidantes e de água Maste thesis, Coimbra: University of Coimbra; 2016, http://hdl.handle.net/10316/37917.
[10] Khan WA, Blobe GC, Hannun YA. Activation of protein-kinase-c by oleic-acid – determination and analysis of inhibition by detergent micelles and physiological membranes – requirement for free oleate. J Biol Chem 1992;267(6):3605–12.
[11] Nishikawa M, Kimura S, Akaike N. Facilitatory effect of docosahexaenoic acid on N-Methyl-D-Aspartate response in pyramidal neurons of rat cerebral-cortex. J Physiol-Lond 1994;475(1):83–93. http://dx.doi.org/10.1113/jphysiol.1994.sp020051.
[12] Liu WS, Heckman CA. The sevenfold way of PKC regulation. Cell Signal 1998;10(8):529–42. http://dx.doi.org/10.1016/s0898-6568(98)00012-6.
[13] Sweatt JD. Toward a molecular explanation for long-term potentiation. Learn Memory 1999;6(5):399–416. http://dx.doi.org/10.1101/lm.6.5.399; Curr Biol. 2014;24(10):R453-R462. http://dx.doi.org/10.1016/j.cub.201403034.
[14] Schieber M, Chandel NS. ROS function in redox signaling and oxidative stress, 24(10) 2014, pp. R453-62. http://dx.doi.org/10.1016/j.cub.2014.03.034.
[15] Melody A, Yodice R, Boone E. Process for producing highly pure oleic acid by hydrolysis of sunflower oil. 1995, Patent EP0349606B1.
[16] Ruiz M, Arias J, Gallardo V. Skin creams made with olive oil. In: Preedy VR, Watson RR, editors. Olives and olive oil in health and disease prevention. Amsterdam: Academic Press; 2010, p. 1133–41. http://dx.doi.org/10.1016/B978-0-12-374420-3.00124-8.
[17] Alves M, Pereira M, Sousa D, Carvakeiro A, Picavet M, Smidt H, et al. Waste lipids to energy: how to optimize methane production from long-chain fatty acids (LCFA). Microb Biotechnol 2009;2(5):538–50. http://dx.doi.org/10.1111/j.1751-7915.2009.00100.x.
[18] Cardoso A, Neves S, Silva M. Esterification of oleic acid for biodiesel production Catalyzed by SnCl2: A kinetic investigation. Energies 2008;1(2):79–92. http://dx.doi.org/10.3390/en1020079.
[19] Emad S. A review of selected non-edible biomass sources as feedstock for biodiesel production, in biofuels - status and perspective. 2015, http://dx.doi.org/10.5772/59178.
[20] Brooke SM, Trafton JA, Sapolsky RM. Autofluorescence as a confound in the determination of calcium levels in hippocampal slices using fura-2AM dye. Brain Res 1996;706(2):283–8. http://dx.doi.org/10.1016/0006-8993(95)01209-5.
[21] Bindokas VP, Jordan J, Lee CC, Miller RJ. Superoxide production in rat hippocampal neurons: Selective imaging with hydroethidine. J Neurosci 1996;16(4):1324–36.
[22] Massaad CA, Klann E. Reactive oxygen species in the regulation of synaptic plasticity and memory. Antioxid Redox Signal 2011;14(10):2013–54. http://dx.doi.org/10.1089/ars.2010.3208.
[23] Duchen MR. Ca2+-dependent changes in the mitochondrial energetics in singledissociated mouse sensory neurons. Biochem J 1992;283:41–50.
[24] Brennan AM, Connor JA, Shuttleworth CW. NAD(P)H Fluorescence transients after synaptic activity in brain slices: Predominant role of mitochondria function. J Cereb Blood Flow Metab 2006;26:1389–406. http://dx.doi.org/10.1038/sj.jcbfm.9600292.
[25] Bartolomé F, Abramov AY. Measurement of mitochondrial NADH and FAD autofluorescence in live cells. Methol Mol Biol 2015;1264:263–70. http://dx.doi.org/10.1007/978-1-4939-2257-4_23.
[26] Sensi SL, Ton-That D, Sullivan PG, Jonas EA, Gee KR, Kaczmarek LK, Weiss J H. Modulation of mitochondrial function by endogenous Zn2+ pools. Proc Natl Acad Sci USA 2003;10:6157–62. http://dx.doi.org/10.1073/pnas.1031598100, PMID: 12724524.
[27] Sensi SL, Paoletti P, Bush AI, Sekler I. Zinc in the physiology and pathology of the CNS. Nat Rev Neurosci 2009;10(11):780–91. http://dx.doi.org/10.1038/nrn2734.
[28] Shuttleworth CW, Weiss JH. Zinc: new clues to diverse roles in brain ischemia. Trends Pharmacol Sci 2011;32:480–6. http://dx.doi.org/10.1016/j.tips.2011.04.001.
[29] Murakami K, Routtenberg A. Direct activation of purified protein kinase-C by unsaturated fatty-acids (oleate and arachidonate) in the absence of phospholipids and Ca2+. Febs Lett 1985;192(2):189–93. http://dx.doi.org/10.1016/0014-5793(85)80105-8.
[30] Freeman D, Petralia R, Wang YX, Mattson M, Yao P. Mitochondria in hippocampal presynaptic and postsynaptic compartments differ in size as well as intensity. J Matters 2017. http://dx.doi.org/10.19185/matters.201711000009.